Modeling of Measurement-based Quantum Network Coding on IBM Q Experience

by

Poramet Pathumsoot

Submitted to the Department of Physics, Faculty of Science
in partial fulfillment of the requirements for the degree of

Bachelor of Science in Physics

at the

MAHIDOL UNIVERSITY

May 2020

Author .....
Department of Physics, Faculty of Science
May 25, 2019

Accepted by .....
Asst. Prof. Sujin Suwanna, Ph.D.
Advisor

Modeling of Measurement-based Quantum Network Coding on IBM Q Experience

by

Poramet Pathumsoot

Submitted to the Department of Physics, Faculty of Science
on May 25, 2019, in partial fulfillment of the
requirements for the degree of
Bachelor of Science in Physics

Abstract

Quantum communication is an important achievement of quantum technology, and the quantum network is an ultimate goal. A network of quantum devices such as qubits or quantum computers can yield interesting properties and potentials that should be optimized, for instance, to overcome a bottleneck network for quantum teleportation. Quantum network coding has been proposed to improve resource utilization to support distributed computation but has not yet been put in to practice. In terms of fundamental research, we investigate a particular implementation of quantum network coding using measurement-based quantum computation on IBM Q processors and compare the performance of quantum network coding with entanglement swapping and entanglement distribution via linear cluster states. We demonstrate the suitability of noisy intermediate-scale quantum (NISQ) devices such as IBM Q for the study of quantum networks and identify the factors that limit the performance of quantum network coding on these processors and provide estimates or error rates required to boost the final Bell pair fidelities to a point where they can be used for generation of genuinely random cryptographic keys among other useful tasks. In terms of software development, the concept of measurement-based quantum network coding has been implemented on classical computers employing local Pauli measurements. A created software can generate a random network of 1-200 nodes with initial resource or quantum network of cluster states. The software can analyze the network connectivity, shortest paths between two nodes using Dijkstra algorithm as well as add or remove nodes or edges. as well as to create entangled pairs of nodes in the network. When Pauli X, Y and Z measurement operators act locally on specific nodes, a subgraph of resulting network of entangled cluster states is shown. Our software can be used to analyze the architect of a quantum network of qubits or quantum computers, which will be tremendously beneficial in quantum communication technology.

Acknowledgments

My life has began when I chose a path of a scientist. The choice is not a gamble; it is nevertheless my dream. First and foremost, I would like to acknowledge my heart for fighting against distraction and social norm, and perseverance to keep this dream to this point. I also would like to leave this message to myself in the future and hope that my heart will forever remain the same.

To be able to earn a scholarship for short-term research in Japan and use a quantum computer, this step of my dream would not be possible without support of my advisors. I would like to express my deepest appreciation to professors Sujin Suwanna and Rodney Van Meter for giving me a chance to work on this project. A piece of scientific work requires so much effort and teamwork behind the scene. I am thankful for financial support from the Honors Program, Faculty of Science, Mahidol University. I thank all my colleagues at Mahidol University and Keio University for all the discussion, sharing and friendship.

From my first year to the last year, I would like to thank to all of my friends, who always encouraged me and listened to me every time I needed. I would like to extend my sincere thanks to everyone in Japan which helped me during my short-term research.

Last but not least, I owe my deepest gratitude to my mother who understands and supports me on this path. Thank you Mom for always pushing me forward, and I love you.

Contents

List of Figures

List of Tables

Chapter 1

Introduction

1.1 Motivation on Quantum Networking

The Dream of realizing quantum internet seem to be far apart in the next decade. However, the revolution coming with could change our lives forever. The essence of quantum communication is to be able to transfer high-quality quantum information from one place to another. In order to sent quantum information represented by quantum bit i.e. qubit flying through the blue sky, Photon qubit becomes the best candidate out of others because it can operate at room temperature. Nevertheless, the noise can still degenerate the quality of the qubit along the way. Due to the No-cloning theorem which not allows us to make an independent copy of quantum information, the classical way of making a copy between the way to the destination for purifying and preserving information is impossible. Nonetheless, the temptation of applications coming along, e.g. quantum cryptography and superdense coding leave the researcher no choice than to move forward on this path. Quantum repeater is proposed [2, 4, 12, 7, 5] to overcome the problems. Entangle link is establish along with a possible purification and error correction from quantum repeater nodes between source to destination nodes. However, a similar problem in classical network also incurs in quantum network which is a contention problem. If the capacity of the route from multiple sources to multiple destinations is limit i.e. the demand of the route is less than supply of the route, it will take longer time to complete the

connection between nodes.

Measurement-based quantum network coding (MQNC) [8] is one of the protocol that can overcome a contention problem by using the idea of measurement-based quantum computing [10]. Apparently, Pauli-measurements on cluster state can resulting in a new topological cluster state which can be easily turn into Bell-pair, the entangle quantum state that application in quantum communication heavily depended. Here, we investigate performance of MQNC on superconducting qubits quantum processor and effect of the noise on the protocol using simulation.

1.2 Organization

The content of this project report is organized as follow. The background required for this project is provided in 2. The implementing result on superconducting qubits quantum computer and noisy simulation are present in 3. Following by Quantum Network Analyzer software using graph theory is in 4. Finally, results are discuss in 5.

Chapter 2

Background Theory

2.1 An introduction tale to Quantum Mechanics

In this section, we will bring you through a concept idea of quantum mechanics and how does it work.

2.1.1 Conceptual Idea

A well known a story of a cat in the box is a Schrödinger's attempt to describe the probabilistic nature of quantum mechanics by torture a kawaii cat. If the Schrödinger's cat is not clarify a thing or two enough then we would like to make an attempt too.

Back in late 18th century, physicist believe that we can describe everything in the universe with Newton's physics known as classical mechanics. However, when they have done experiment about smaller thing, they become aware that their beloved classical mechanics cannot explain why small thing behaves like this. Double slit experiment is a prime example of such a quantum phenomena.

The double-slit experiment is an experiment where electrons being shot through a double-slit before a background. Classically, we would expect that the pattern should look like a gunshot on the background. Surprisingly, electron shots produce an interference pattern like a wave. Nevertheless, if we take a peek at which hole do electrons

pass-through, then the pattern behaves like what we would classically expect. This strange behavior of electron was later found to be a wave-particle duality property of a quantum object. In order to predict the behavior and properties of an object, one needed an equation of motion of the object which obeys Newton's law. Similar to classical mechanics, to describe a quantum object, one needed 'wave function.' of quantum objects, which obeys Schrodinger's equation. The difference is that the wave function usually describes the probability amplitude of the quantum object being in a specific state as a superposition of every possible outcome. If the wave function is left undisputed, then when a quantum object got change by quantum operation, a resulting wave function will be the superposition of every possible outcome, which one outcome may interfere with others. However, if the wave function is disrupted by 'measurement,' the wave function will 'collapse,' left with only particular possible outcomes. The action of 'take a peek.' is a measurement, which responsible for the collapse of a wave function.

2.1.2 Mathematics formulation

A mathematics formulation capable of describe quantum mechanics, specifically in quantum computing is a Dirac bra-ket notation formulation. For example, consider orthogonal two-level system of quantum object in the wave function form of *ket*,

$$|\psi\rangle = \alpha|0\rangle + \beta|1\rangle, \tag{2.1}$$

where α and β are probability amplitude of state $|0\rangle$ and $|1\rangle$ respectively. The *bra* form of equation 2.1 is complex conjugate of *ket*,

$$\langle\psi| = \alpha^*\langle 0| + \beta^*\langle 1| \tag{2.2}$$

Since α and β are probability amplitude then they should obey a normalization condition in order to conserve the probability as $|\alpha|^2 + |\beta|^2 = 1$. The calculation

of bra-ket notation are follow,

$$\begin{aligned} \langle\psi|\psi\rangle &= (\alpha^*\langle 0| + \beta^*\langle 1|)(\alpha|0\rangle + \beta|1\rangle) \\ &= \alpha^*\alpha\langle 0|0\rangle + \alpha^*\beta\langle 0|1\rangle + \beta^*\alpha\langle 1|0\rangle + \beta^*\beta\langle 1|1\rangle \\ 1 &= |\alpha|^2 + |\beta|^2. \end{aligned} \tag{2.3}$$

As an orthogonal basis, $\langle m|n\rangle = 1$ if $m = n$ and $\langle m|n\rangle = 0$ if $m \neq n$. Equation 2.1 reveal to us a superposition of state $|0\rangle$ and $|1\rangle$ which are possible outcomes of measurement the wave-function in Z basis. Consider the case where $\alpha = \beta = \frac{1}{\sqrt{2}}$ then, if we prepare this quantum state for one hundred sample and measure them, we would observe that it will be $|0\rangle$ for fifty of the times.

The Dirac's bra-ket notation in the vector form defined as

$$|0\rangle \equiv \begin{bmatrix} 1 \\ 0 \end{bmatrix}, |1\rangle \equiv \begin{bmatrix} 0 \\ 1 \end{bmatrix}, \langle 0| \equiv \begin{bmatrix} 1 & 0 \end{bmatrix}, \langle 1| \equiv \begin{bmatrix} 0 & 1 \end{bmatrix} \text{ thus } |\psi\rangle \equiv \begin{bmatrix} \alpha \\ \beta \end{bmatrix}, \tag{2.4}$$

which usually refer as computational basis or Pauli Z basis. For Pauli X and Y, they defined as

$$|+\rangle \equiv \frac{1}{\sqrt{2}} \begin{bmatrix} 1 \\ 1 \end{bmatrix}, |-\rangle \equiv \frac{1}{\sqrt{2}} \begin{bmatrix} 1 \\ -1 \end{bmatrix}, \tag{2.5}$$

and

$$|+i\rangle \equiv \frac{1}{\sqrt{2}} \begin{bmatrix} 1 \\ i \end{bmatrix}, |-i\rangle \equiv -\frac{1}{\sqrt{2}} \begin{bmatrix} 1 \\ -i \end{bmatrix}. \tag{2.6}$$

We can describe a system of many quantum objects using tensor products, for example, consider a system of two two-level system A and B,

$$A = \begin{bmatrix} a_0 \\ a_1 \end{bmatrix}, B = \begin{bmatrix} b_0 \\ b_1 \end{bmatrix}. \tag{2.7}$$

The composite system,

$$A \otimes B = \begin{bmatrix} a_0 \begin{bmatrix} b_0 \\ b_1 \end{bmatrix} \\ a_1 \begin{bmatrix} b_0 \\ b_1 \end{bmatrix} \end{bmatrix} = \begin{bmatrix} a_0 b_0 \\ a_0 b_1 \\ a_1 b_0 \\ a_1 b_1 \end{bmatrix}. \tag{2.8}$$

In order to describe mixed state, we use density matrix which defined as,

$$\begin{aligned} |\psi\rangle\langle\psi| &= \begin{bmatrix} \alpha \\ \beta \end{bmatrix} \begin{bmatrix} \alpha^* & \beta^* \end{bmatrix} \\ |\psi\rangle\langle\psi| &= \begin{bmatrix} |\alpha|^2 & \alpha\beta^* \\ \alpha^*\beta & |\beta|^2 \end{bmatrix} \end{aligned} \tag{2.9}$$

2.1.3 Entanglement

Entanglement is a state where composite quantum system cannot write as tensor product of subsystem. In other word, the action on quantum object will immediately affect other. For example consider simple two quantum objects which take a form similar to equation 3.1,

$$|\Phi^+\rangle = \frac{1}{\sqrt{2}}(|00\rangle + |11\rangle). \tag{2.10}$$

The equation 2.10 is one of the famous *Bell pair*. Measuring one of the quantum object will collapse the entire wave function which the remaining state show us that the another quantum object will also be determined. In other word if the measuring result of the first quantum object is in state $|0\rangle$ then the another will also be in state $|0\rangle$ while if the result of first object is $|1\rangle$ then the another is also state $|1\rangle$. Furthermore, Bell pair also have other form which can use as Bell basis, which those

basis are defined as,

$$|\Phi^+\rangle = \frac{1}{\sqrt{2}}(|00\rangle + |11\rangle), \tag{2.11}$$

$$|\Phi^-\rangle = \frac{1}{\sqrt{2}}(|00\rangle - |11\rangle), \tag{2.12}$$

$$|\Psi^+\rangle = \frac{1}{\sqrt{2}}(|01\rangle + |10\rangle), \tag{2.13}$$

$$|\Psi^-\rangle = \frac{1}{\sqrt{2}}(|01\rangle - |10\rangle). \tag{2.14}$$

Another entangle form which used in measurement-based quantum computing and network coding is cluster state. A Simple form of cluster state is,

$$|G_2\rangle = \frac{1}{2}(|00\rangle + |01\rangle + |10\rangle - |11\rangle), \tag{2.15}$$

where the entanglement lie in the global phase of the state $|11\rangle$.

2.1.4 Fidelity

To quantify the closeness of two quantum states, the fidelity,

$$F(\rho, \sigma) = \left[\mathrm{Tr}\left\{\sqrt{\sqrt{\rho}\sigma\sqrt{\rho}}\right\}\right]^2, \tag{2.16}$$

is often used for density matrix ρ and σ. If fidelity $F(\rho, \sigma) = 1$ then ρ is identical to state σ. The fidelity can be reduce to,

$$F(\rho, \sigma) = \langle\psi|\rho|\psi\rangle, \tag{2.17}$$

where $\sigma = |\psi\rangle\langle\psi|$ and ψ is a pure state.

2.2 Quantum Communication and Computing

No-cloning theorem is a heart of quantum communication. There is no way to make a copy of independent unknown quantum state which make quantum commu-

nication achieve the next-level of security. While superposition property of quantum state allow quantum computing to calculate every possible input at the very same time, however the answer still, nevertheless, in superposition which mean that we will obtain random answer from measurement. The job of quantum physicist is to figuring out how to obtain useful answer from the outcome quantum state. In this section, we will explore how to use quantum state for computation and communication task. Fortunately, quantum computing and quantum communication are using the very same fundamental concept.

2.2.1 Qubit

Comparing to classical computer, the smallest unit of quantum computer called 'qubits'. Qubit can be any quantum object that can be treat as two-level system as in equation 2.1.

2.2.2 Quantum Operation

As a building block of quantum operation, quantum logic gate is also necessary to manipulate quantum state storing in qubits as how classical computing is done by classical logic gate. There are many universal sets of quantum logic gate required to compute any computation task. Here, we present selected useful quantum gates.

The very first quantum gate we excited to introduce is Hadamard gate defined in matrix form as

$$H = \begin{bmatrix} 1 & 1 \\ 1 & -1 \end{bmatrix}. \tag{2.18}$$

Hadamard gate usually used to initialize superposition of the inputs and make a change of basis for X-basis measurement. X gate is comparable to NOT logic gate

$$|0\rangle \text{ ——} \boxed{H} \text{——} \ \tfrac{1}{\sqrt{2}}(|0\rangle + |1\rangle)$$

$$|1\rangle \text{ ——} \boxed{H} \text{——} \ \tfrac{1}{\sqrt{2}}(|0\rangle - |1\rangle)$$

Figure 2-1: Examples of how Hadamard gate affect input quantum state.

in classical. While classical bit have only bit flip, qubit also have phase rotation operation as Z gate and the combination of them, $Y = XZ$.

$$X = \begin{bmatrix} 0 & 1 \\ 1 & 0 \end{bmatrix}, Z = \begin{bmatrix} 1 & 0 \\ 0 & -1 \end{bmatrix}, Y = \begin{bmatrix} 0 & -i \\ i & 0 \end{bmatrix}. \tag{2.19}$$

Hadamard gate usually used to initialize superposition of the inputs and make a change of basis for X-basis measurement.

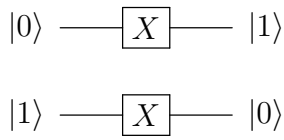

(a) Examples of how X gate affect input quantum state.

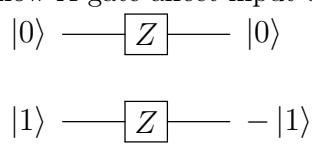

(b) Examples of how Z gate affect input quantum state.

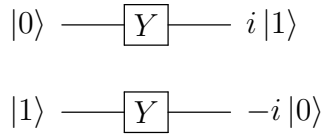

(c) Examples of how Y gate affect input quantum state.

Figure 2-2: Example of how Pauli gates affect input state

As for general unitary operator $U(\theta, \phi, \lambda)$ defined as

$$U(\theta, \phi, \lambda) = \begin{bmatrix} \cos(\theta/2) & -e^{i\lambda}\sin(\theta/2) \\ e^{i\phi}\sin(\theta/2) & e^{i\lambda+i\phi}\cos(\theta/2) \end{bmatrix}, \tag{2.20}$$

where $0 \leq \theta \leq \pi$, $0 \leq \phi \leq 2\pi$ and $0 \leq \lambda \leq 2\pi$. The another type of quantum gate that important for quantum computing is two-qubits gate. Without two-qubits gate that create an entanglement between qubits, quantum computing would no different to classical computing with fantasy bit. The two-qubits quantum gate usually has one qubit act as control qubit while another qubit being controlled. A simplest form

of a two-qubits gate is controlled-X gate defined as

$$C_x = \begin{bmatrix} 1 & 0 & 0 & 0 \\ 0 & 0 & 0 & 1 \\ 0 & 0 & 1 & 0 \\ 0 & 1 & 0 & 0 \end{bmatrix}. \tag{2.21}$$

Controlled-X gate flips target qubit if the control qubit is in state $|1\rangle$ and do nothing otherwise as illustrate in figure 2-3.

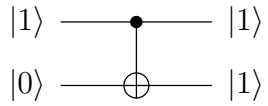

(a) Simple illustrate of how controlled-X affect input state

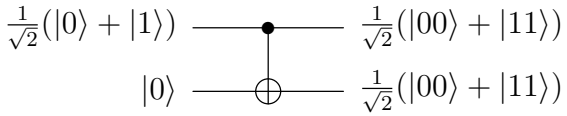

(b) Illustrate of how controlled-X affect superposition input state such that its create entanglement between qubits

Figure 2-3: Example of a controlled-X gate.

The general form of two-qubits gate defined as

$$C_{u3}(\theta,\phi,\lambda) \equiv \begin{bmatrix} 1 & 0 & 0 & 0 \\ 0 & e^{-i(\phi+\lambda)/2}\cos(\theta/2) & 0 & -e^{-i(\phi-\lambda)/2}\sin(\theta/2) \\ 0 & 0 & 1 & 0 \\ 0 & e^{i(\phi-\lambda)/2}\sin(\theta/2) & 0 & e^{i(\phi+\lambda)/2}\cos(\theta/2) \end{bmatrix}. \tag{2.22}$$

The two-qubits quantum gate that is important for this work is controlled=Z gate, which require for create a cluster state entangle. Controlled-Z gate defined as

$$C_Z = \begin{bmatrix} 1 & 0 & 0 & 0 \\ 0 & 1 & 0 & 0 \\ 0 & 0 & 1 & 0 \\ 0 & 0 & 0 & -1 \end{bmatrix}. \tag{2.23}$$

The preparation of cluster state including Hadamard gate and controlled-Z gate,

$$\begin{aligned} |\psi_1\rangle = H \otimes H|0\rangle|0\rangle &= \frac{1}{2}(|00\rangle + |01\rangle + |10\rangle + |11\rangle) \\ |\psi_2\rangle = C_Z|\psi_1\rangle &= \frac{1}{2}(|00\rangle + |01\rangle + |10\rangle - |11\rangle). \end{aligned} \tag{2.24}$$

This can easily seen that linear cluster state can be turn into bell pair using addition Hadamard gate on either qubits,

$$H \otimes I|\psi_2\rangle = \frac{1}{\sqrt{2}}(|00\rangle + |11\rangle). \tag{2.25}$$

Furthermore, Cotrolled-X gate can be decompose into controlled-Z and Hadamard gates as follow in figure 2-4

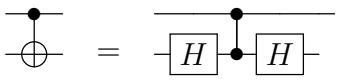

Figure 2-4: Decomposition of Controlled-X using Controlled-Z and two Hadamard gates

2.3 Quantum States on a Network and Operations

As a quantum network is a network of quantum devices, we need to study information teleportation on a network. A network can be represented mathemtically as a graph, where the devices act as nodes on the graph. In a practical sense, a quantum network can be a network of qubits, which constitute a processor such as thoses of IBM, Google, Regetti or other leading quantum technology companies. A network can also be a network of quantum computers linked remotely; maybe these quantum computers are located in different countries. Nevertheless, the mathematical description of a network will be the same, and the operations on the network will be similar. In this section, for completeness, we provide the basics for a quantum network focusing on a network graph state and local operations.

A graph is a set of nodes or vertices V together with a set of edges E, and instruction how the nodes are connected. In a quantum network an edge could have double

meaning; one simply implies a connection between two nodes (e.g. two devices, or two qubits), while the other has stronger requirement as it signifies the entanglement between the two connecting nodes.

For a quantum network, it is a natural to think of a network itself as a quantum entity, and therefore, it should have its own quantum states. Borrowing insights from many-particle systems, a quantum state of the entire network should be constructed from composite states of its own elements, leading to a tensor product of states. This is called a *cluster state*. By default, then the overall Hilbert space of a quantum network state is given by the tensor product of Hilbet spaces of individual Hilbert spaces corresponding to each device (we implicitly assume that there are finite number of nodes, i.e. quantum devices, in a network). Consequently, an operation on a network state, or graph state, consists of local operation at each node (including the identity operation), and can be expressed in the form a tensor product as well.

2.3.1 Relevant Graph Theory and Terminology

A graph is denoted by $G = (V, E)$, where V is a set of vertices and E is a set of edges. Here, we assume that V is a finite set, which can be enumerated as $V = \{1, 2, ..., N\}$, and $E \subset V \times V$ denotes a set of connection from a subset of V to a subset of V. Let lower-case letters denote vertices, e.g. $a, b \in V$; then a pair $\{a, b\}$ denotes an edge in E which connects the vertices a and b.

For each vertex $a \in V$, we can define a neighborhood of a as

$$N_a = \{b \in V : \{a, b\} \in E\}, \tag{2.26}$$

i.e. a neighborhood of a is a set of vertices connected to a by edges. By default, $N_a = \varnothing$, the empty set when a is isolated in G.

When a vertex a is deleted in a graph G, all the edges connecting to a will be removed, resulting in a new graph, which will be denoted by $G \setminus a$. If U is a subset of vertices, i.e. $U \subset V$, of a graph $G = (V, E)$, we denote by $G \setminus U$ the graph that is obtained from G after deleting all the vertices in the set U, and all corresponding

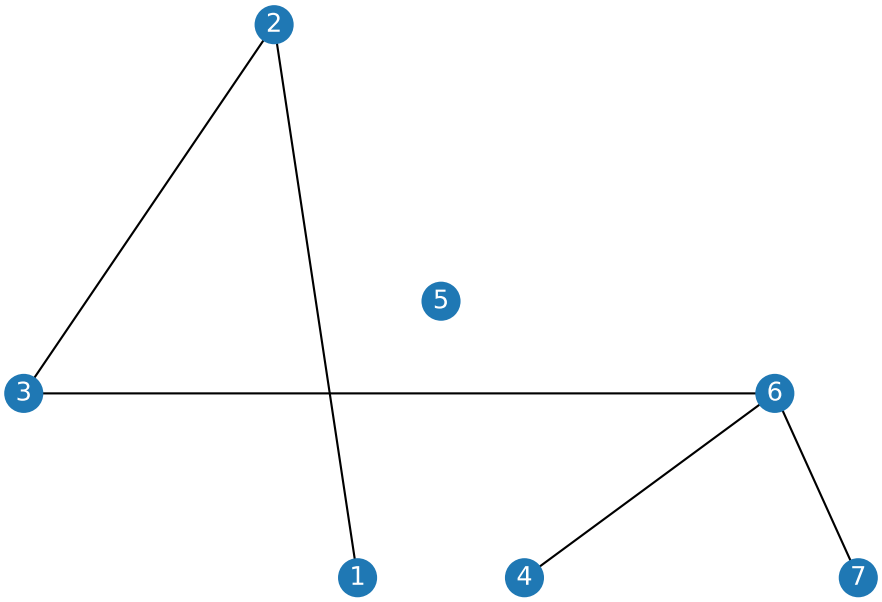

Figure 2-5: An example of a graph with seven vertices and five edges.

edges with elements of U. Similarly, if F is a subset of vertices, i.e. $F \subset E$, then $G \setminus F$ denotes a resultant graph after removing all edges in F.

For addition of edges, we have $G \cup F = (V, E \cup F)$ and $G + F = (V, E + F)$, where $A + B$ denotes a symmetric addition of two sets:

$$A + B = (A \cup B) \setminus (A \cap B) \tag{2.27}$$

Let $A \subset V$, then an induced *subgraph* $G[A]$ is obtained by deleting all vertices that are not contained in A, together with all the incident edges to A.

As for local operations on a graph, there are two basis operations, namely, a deletion of a vertex, and a local complementation of a vertex. This follows from the action of local Clifford operations on graph states [1]. The local complementation at $a \in V$, denoted by $\tau_a(G)$, is obtained by complementing the subgraph of G induced by the neighborhood N_a of a and leaving the rest of the graph unchanged. Precisely,

$$\tau_a G :\mapsto \tau_a(G) = G + N_a. \tag{2.28}$$

As an illustration, examples of local complementation on a graphs are shown in

Figure 2-6a.

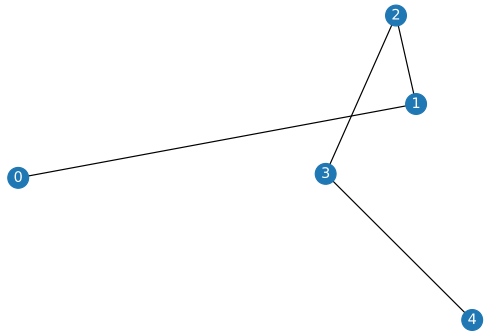

(a) Initial resource

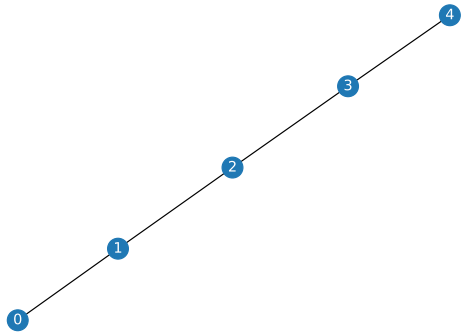

(b) local complementation on node 0

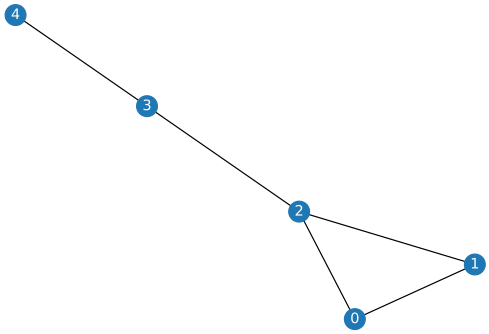

(c) local complementation on node 1

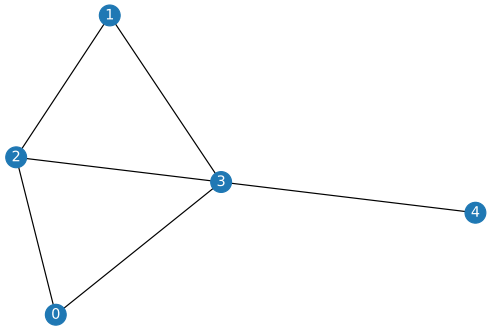

(d) local complementation on node 2

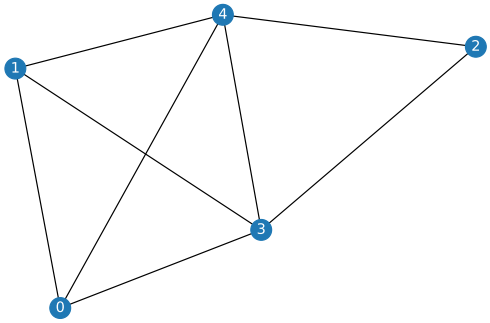

(e) local complementation on node 3

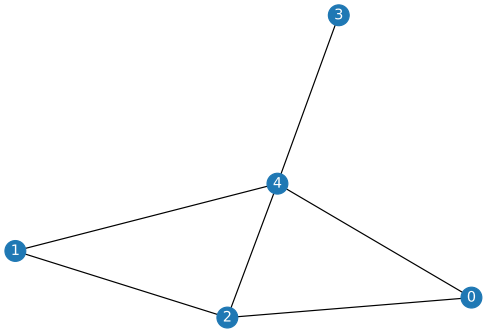

(f) local complementation on node 4

Figure 2-6: local complementation on nodes

2.3.2 Graph State

Let us consider a set of 2-level systems (qubits) that are labeled by the vertices V of a graph G. We suppose that the qubits are prepared in some initial state vector $|\psi\rangle$ and then are coupled according to some interaction pattern represented by the connecting edges of the graph G. For $\{a, b\} \in E$, the qubits of the two connected

vertices a and b interact with the Hamiltonian H_{ab}. Hence, the evolution of the state is according to some (non-local) unitary operator

$$U_{ab} = e^{-i\varphi_{ab}} H_{ab}, \tag{2.29}$$

where φ_{ab} indicates the coupling strength or (with appropriate physical units) the interaction time.

To construct operations on a quantum network, for simplicity, we assume that the network consists of qubits as its nodes. The space of operators on a qubit can be spanned the Pauli matrices together with the 2×2 identity matrix. Let σ_x, σ_y and σ_z denote the Pauli matrices, and let $|0\rangle$ and $|1\rangle$ denote the eigenvectors of σ_z corresponding to the eigenvalues $+1$ and -1, respectively. We use the superscript to denote the quantum state at node a, for instances, σ_z^a or $\mathbf{1}^a$ denote the Pauli σ_a operator or the identity operator at node a.

When U is a subset of nodes, the overall quantum state of a quantum network whose nodes form the set U is given by a tensor product. For example,

$$|+\rangle^U = \bigotimes_{a \in U} |+\rangle^a. \tag{2.30}$$

Here, as usual, $|\pm\rangle = (1/\sqrt{2})[|0\rangle \pm |1\rangle]$ Similarly, a operator on a network of nodes is given by a tensor product, e.g.

$$\sigma_y^U = \bigotimes_{a \in U} \sigma_y^a. \tag{2.31}$$

Let $\mathcal{P}^a$ denote a local operator at node a, e.g. $\mathcal{P}^a$ can be any linear combination of $\mathbf{1}, \sigma_x, \sigma_y$ and σ_z, then can operator on a quantum network U is defined as

$$\mathcal{P}^U = \bigotimes_{a \in U} \mathcal{P}^a. \tag{2.32}$$

When we consider a quantum state on a network or graph, it is called a *graph state*, which is in fact a cluster of quantum states, so sometimes it is also called a *cluster state*, with only a slight difference that a cluster state does not need an

underlying graph structure. A graph state of a quantum network can be viewed from the interaction between nodes, i.e. the operators U_{ab} can be utilized to construct a graph state.

Let $G = (V, E)$ be a graph. Then, the graph state $|G\rangle$ of a graph G is the pure state with state vector

$$|G\rangle = \prod_{\{a,b\}\in E} U_{ab}|+\rangle^V. \tag{2.33}$$

A physical interpretation of the graph state $|G\rangle$ is that the qubit at each vertex is prepared in the pure state with state vector $|+\rangle$ as eigenvector of σ_x with eigenvalue $+1$. Then the interaction is applied via U_{ab} which is equivalent to mixing the phase gate to all vertices a, b that are adjacent in G.

2.3.3 Pauli Measurement on Graph State

With the Pauli matrices, we will frequently use the projectors onto the eigenvectors of the Pauli operators. These are defined as

$$P^a_{x,\pm} = \frac{1 \pm \sigma^a_x}{2}, \tag{2.34}$$

$$P^a_{y,\pm} = \frac{1 \pm \sigma^a_y}{2}, \tag{2.35}$$

$$P^a_{z,\pm} = \frac{1 \pm \sigma^a_z}{2}. \tag{2.36}$$

These Pauli measurement operators can act on a cluster state $|G\rangle$, and it can compose of local operations on a graph, i.e. a deletion and local complementation [6].

In summary, a Pauli measurements on node correspond to a certain sequence of local complementation on node. For examples, if σ_x, σ_y and σ_z act on a node a, they are equivalent to

$\sigma_z \equiv$ deleting a node a from G

$\sigma_y \equiv$ performing local complementation on a node a and deleting node a from G

$\sigma_z \equiv$ choosing any node b that connects to node a, then performing local complementation on node b, following by local complementation on node a, and removing

node a from G, and lastly, perfoming a local complementation on node b.

Consequently, the local Pauli operations can be expressed algebraically as

$$P^a_{z,\pm}|G\rangle = \frac{1}{\sqrt{2}}|z,\pm\rangle^a \otimes U^a_{z,\pm}|G-a\rangle \tag{2.37}$$

$$P^a_{y,\pm}|G\rangle = \frac{1}{\sqrt{2}}|y,\pm\rangle^a \otimes U^a_{y,\pm}\,|\tau_a(G)-a\rangle \tag{2.38}$$

$$P^a_{x,\pm}|G\rangle = \frac{1}{\sqrt{2}}|x,\pm\rangle^a \otimes U^a_{x,\pm}\,|\tau_{b_0}\left(\tau_a\circ\tau_{b_0}(G)-a\right)\rangle\,, \tag{2.39}$$

where the operator U^a_P is corresponding to each Pauli measurement as,

$$U^a_{z,+} = \mathbf{1} \quad , \qquad U^a_{z,-} = \sigma_z^{N_a} \tag{2.40}$$

$$U^a_{y,+} = \sqrt{-i\sigma_z}^{N_a} \quad , \qquad U^a_{y,-} = \sqrt{+i\sigma_z}^{N_a} \tag{2.41}$$

$$U^a_{x,+} = \sqrt{+i\sigma_y^{b_0}}\,\sigma_z^{N_a\setminus\left(N_{b_0}\cup b_0\right)} \quad , \quad U^a_{x,-} = \sqrt{-i\sigma_y^{b_0}}\,\sigma_z^{N_{b_0}\setminus(N_a\cup a)}. \tag{2.42}$$

2.4 Measurement-based Network Coding (MQNC)

Originally, measurement-based network coding (MQNC) is inspire by measurement-based quantum computing (MBQC) using a cluster state as initial resource which achieve universal quantum gate via sequence of Pauli measurements. The cluster state defined as

$$|G\rangle = \prod_{(a,b)\in E} C_Z^{ab}|+\rangle^{\otimes n}. \tag{2.43}$$

Where $C_Z^{ab} = |0\rangle\langle 0|_a \otimes I_b + |1\rangle\langle 1|_a \otimes Z_b$ is the controlled-Z gate acting on qubits a and b. Pauli measurement is applying in sequence to generate a desire cluster state topology.

Chapter 3

Modeling of Measurement-based Quantum Network Coding on Superconducting qubits Quantum Processor

In order to teleport qubit from one place to another in the network, the simple protocol is entanglement swapping using Bell measurement to create entangle state between apart qubits. While Measurement-based quantum network coding uses Pauli measurement to link unconnected qubits together. Both protocol can be model and implement on a IBM Q's superconducting quantum computers to address performance of each protocol in term of state fidelity.

We have chosen IBM Q 20 Tokyo and IBM Q 20 Poughkeepsie due to their connectivity map in figure[3-1] which suit for implement entanglement swapping and linear cluster state, which is the MQNC where X measurement is performed on inter qubits.

To create two separated crossing-over entangle pairs, instead of begin with 14 qubits initial resource as in [8], we perform the protocol with 6 qubits initial resource due to the limitation of device connectivity.

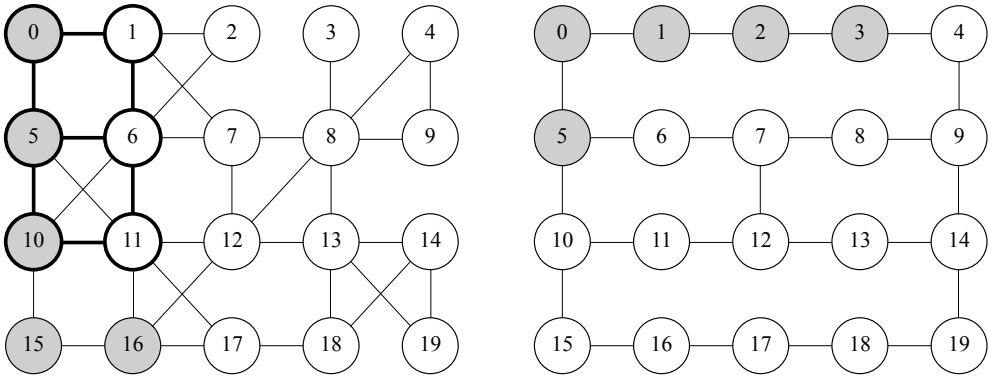

(a) IBM Q 20 Tokyo topology (b) IBM Q 20 Poughkeepsie topology

Figure 3-1: IBM Q superconducting qubits quantum computer connectivity topology [9]

3.1 Entanglement Swapping

Consider a simple situation, two apart qubits needed to be directly connected in the end of the protocol where there are two inter-connect qubits between them as illustrate in figure[3-2a].

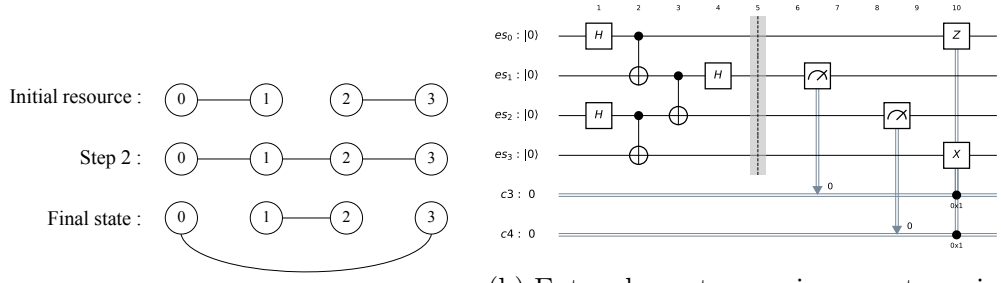

(a) Entanglement swapping scheme (b) Entanglement swapping quantum circuit

Figure 3-2: Entanglement Swapping [9]

Entanglement swapping protocol was being implemented twice on IBM Q 20 Tokyo where qubits the $\{0, 1, 2, 3\}$ are mapped to qubits $\{0, 5, 6, 11\}$ and $\{1, 5, 6, 10\}$ using quantum circuit as in figure [3-2b]. The protocol was implemented for one trial, repeated for 8192 shots (round), and the result where measurement outcome of qubits $\{5, 6\}$ are '0' was used to reconstruct density matrix using state-tomography and then

calculate state fidelity with respect to ideal state,

$$|\Phi^+\rangle = \frac{1}{\sqrt{2}}(|00\rangle + |11\rangle). \tag{3.1}$$

The result where measurement outcome of qubits $\{5, 6\}$ are '0' was selected because that there is no require for addition byproduct operation to correct the state after protocol. The fidelity $F \approx 0.76$ for qubits $\{0, 11\}$ and $F \approx 0.66$ for qubits $\{1, 10\}$.

3.2 Linear Cluster State

In the similar situation as the entanglement swapping protocol, MQNC also capable of connect distant qubits with series of Pauli measurement as illustrate in figure[3-3a].

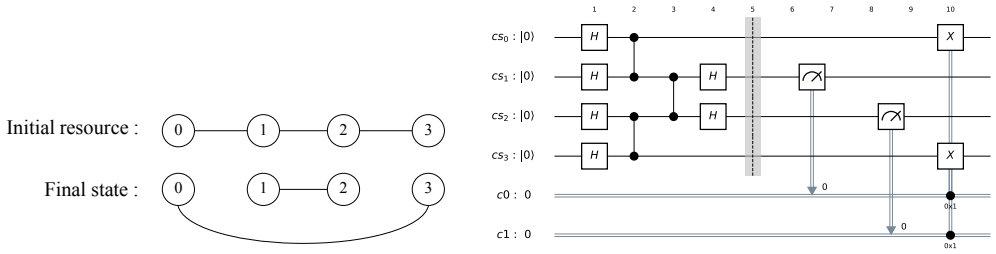

(a) MQNC on linear cluster state scheme

(b) MQNC on linear cluster state quantum circuit

Figure 3-3: MQNC on linear cluster state [9]

We perform MQNC protocol on linear cluster state for 1 trial using IBM Q 20 Tokyo where qubits the $\{0, 1, 2, 3\}$ are mapped to qubits $\{0, 5, 6, 11\}$ and $\{1, 5, 6, 10\}$ using quantum circuit as in figure [3-3b]. The result which measurement outcome of qubits $\{5, 6\}$ are '0' was selected for reconstruct density matrix using state-tomography. The fidelity is then calculate with respect to ideal 2 qubits linear cluster state,

$$|G_2\rangle = \frac{1}{\sqrt{2}}(|0+\rangle + |1-\rangle). \tag{3.2}$$

The fidelity $F \approx 0.70$ for qubits $\{0, 11\}$ and $F \approx 0.63$ for qubits $\{1, 10\}$. The fidelity result from entanglement swapping and MQNC is close to each other, this

is to be expected. Because, source of the noise is mainly coming from two-qubits gate which is the same for implementing on IBM Q devices. Since we need three CZ gate for construct initial resource for MQNC which require linear cluster state while entanglement swapping use two CX gate to initialize resource however, entanglement swapping require Bell measurement which use one addition CX gate to complete the protocol.

3.3 Butterfly Network

In the realistic situation, the network of quantum repeater may link to each other in more complex way which can be resulting in contention during the transmission. A simple demonstration case of such a network is a butterfly network as shown in figure["butterfly network"] where MQNC become useful in this situation.

3.3.1 Implementation on IBM Q devices

The objective is to connect qubits $\{0, 5\}$ and qubits $\{2, 3\}$ as illustrate in figure[3-4a]. To model butterfly network on IBM Q device, we use IBM Q 20 Tokyo as its suitability for initialize 6-qubits cluster state without needing of swapping operation. The qubits used in IBM Q 20 Tokyo are $\{0, 1, 5, 6, 10, 11\}$ corresponding to qubits $\{0, 1, 2, 3, 4, 5\}$ in the figure[3-4a] respectively.

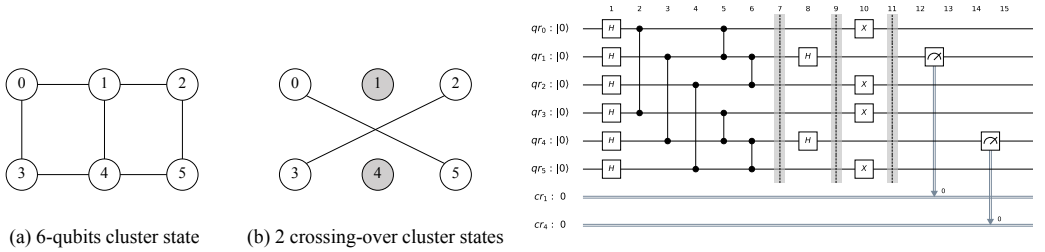

(a) 6-qubits cluster state (b) 2 crossing-over cluster states

(b) MQNC on linear Butterfly network

(a) MQNC on Butterfly network resource quantum circuit

Figure 3-4: MQNC on Butterfly network

Quantum circuit for initialize resource and implement MQNC on IBM Q 20 Tokyo is shown in figure[3-4b]. An initial resource of butterfly network is construct with op-

erations in time-step 1 - 6. Operation in time-step 8 is to change basis for performing the X measurement. Time-step 10 is a byproduct operation to correct the final state where measurement outcome of qubits $\{5, 6\}$ ($\{1, 4\}$ in the quantum circuit) are '1'. We implement the protocol for twenty trial with and reconstruct 4-qubits density matrix using state tomography where the fidelity $F \approx 0.41 \pm 0.01$. We also obtain density matrices of each separated pairs using partial trace where $F \approx 0.57 \pm 0.01$ for qubits $\{0, 11\}$ (figure[3-5c]) and $F \approx 0.58 \pm 0.01$ for qubits $\{1, 10\}$ (figure[3-5d]).

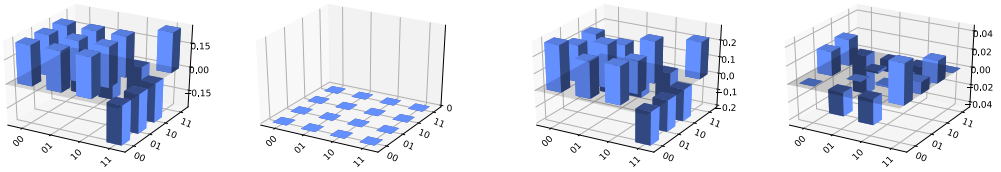

(a) Expected density matrix of 2-qubits linear cluster state

(b) Directly created 2-qubits linear cluster state using neighboring qubits

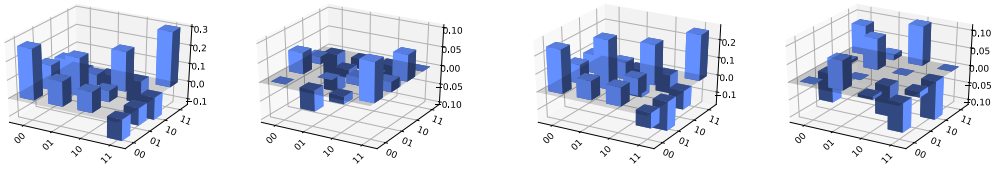

(c) Reconstructed density matrix of qubits $\{0, 11\}$

(d) Reconstructed density matrix of qubits $\{1, 10\}$

Figure 3-5: Density matrices of 2-qubits linear cluster state

3.3.2 Entanglement Verification

In order to investigate the protocol under the current circumstance, we first calculate classical correlation of the created entangled pairs. As shown in figure[3-6], by using QASM simulator, the ideal result should yield maximally correlation for qubits pair $\{0, 11\}$ and $\{1, 10\}$ and zero correlated for other pairs. However, for actual implementation of the protocol, the correlation dropping from the ideal case. Nevertheless, this is to be expected, since the error of preparation, operation and measurement on qubits are exist.

We then now investigate for how are they entangle. Concurrence is a convention

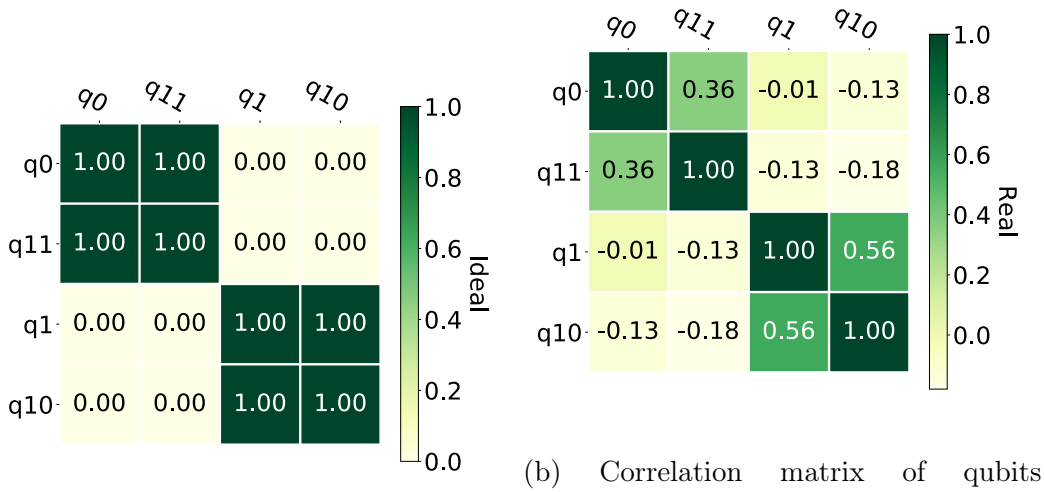

(a) Correlation matrix of ideal Bell pair

(b) Correlation matrix of qubits $\{0, 1, 10, 11\}$ after protocol and turning into Bell pair via H operation

Figure 3-6: MQNC on Butterfly network [9]

way to quantify the entanglement of 2-qubits system. The concurrence defined as

$$C_\rho = \max\{0, \lambda_1 - \lambda_2, \lambda_3, \lambda_4\}, \tag{3.3}$$

where $\lambda_i; i = 1, 2, 3, 4$ are the eigenvalues of R_ρ in the decreasing order. Hermitian matrix $R_\rho = \sqrt{\sqrt{\rho}\tilde{\rho}\sqrt{\rho}}$, $\tilde{\rho} = (Y \otimes Y)\rho^*(Y \otimes Y)$ and Y is Pauli spin matrix.

	pair	$C(\rho)$
Entangled pairs	$\{0, 11\}$	0.253 ± 0.018
	$\{1, 10\}$	0.312 ± 0.021
Separable pairs	$\{0, 10\}$	0
	$\{0, 1\}$	0
	$\{10, 11\}$	0
	$\{1, 11\}$	0

Table 3.1: Concurrence of each qubits pair after protocol

As expected, in table 3.1, the concurrence of the qubits pair that suppose to be non-entangle is zero as they can be separable.

Now, we proceed to investigate on how useful of the created entangle pairs. One of the practical application of the distant entangle pair is to create random cryptography key without any local correlation. CHSH test can be used to verify that if the

produced result has a hidden variable behind the phenomenon or not. The CHSH inequality follow,

$$S = \langle AB \rangle - \langle AB' \rangle - \langle A'B \rangle - \langle A'B' \rangle, \tag{3.4}$$

where $\langle O_1 O_2 \rangle = \mathrm{Tr}\{O_1 O_2 \rho\}$ and $A = H, A' = Z, B = H, B' = ZHZ$.

	pair	S Value
Entangled pairs	$\{0, 11\}$	1.165 ± 0.04
	$\{1, 10\}$	1.235 ± 0.04
Separable pairs	$\{0, 10\}$	-0.405 ± 0.06
	$\{0, 1\}$	-0.149 ± 0.03
	$\{10, 11\}$	-0.326 ± 0.04
	$\{1, 11\}$	-0.084 ± 0.06

Table 3.2: S value of each qubit pair after the protocol using IBM Q 20 Tokyo

We perform the CHSH test for 8 trials using IBM Q 20 Tokyo and post-selected the result where measurement outcome of qubit $\{1, 4\}$ is '1'. Table 3.2 shows S value of each qubit pairs, where the pair that expected to be entangle have significant higher S value than other pairs. However, they fail to violate the CHSH inequality as the value are not exceed 2. This is not surprising as their fidelity suggest the produced result.

3.3.3 Noise modeling using QASM simulation

The imperfect of the devices is responsible for the outcome of the MQNC implementation. We tried to address type of the noise, how strong is it on comparing to the real devices, and how much does the devices need to improve until the protocol can produce the practical result.

We simulated the protocol using Qiskit's QASM simulator which can simulate noisy devices by specify noise model before execution. A simple noise model that we use is depolarizing noise channel defined as,

$$E_O(\rho) = (1 - \epsilon) O \rho O^\dagger + \frac{\epsilon}{2}. \tag{3.5}$$

While, the mixed state of two entangled qubits are modeled as rotated Werner state,

$$\rho^W = \frac{4F-1}{3}|G_2\rangle\langle G_2| + \frac{1-F}{3}I, \tag{3.6}$$

where I is identity operator and F is the fidelity with respect to $|G\rangle$.

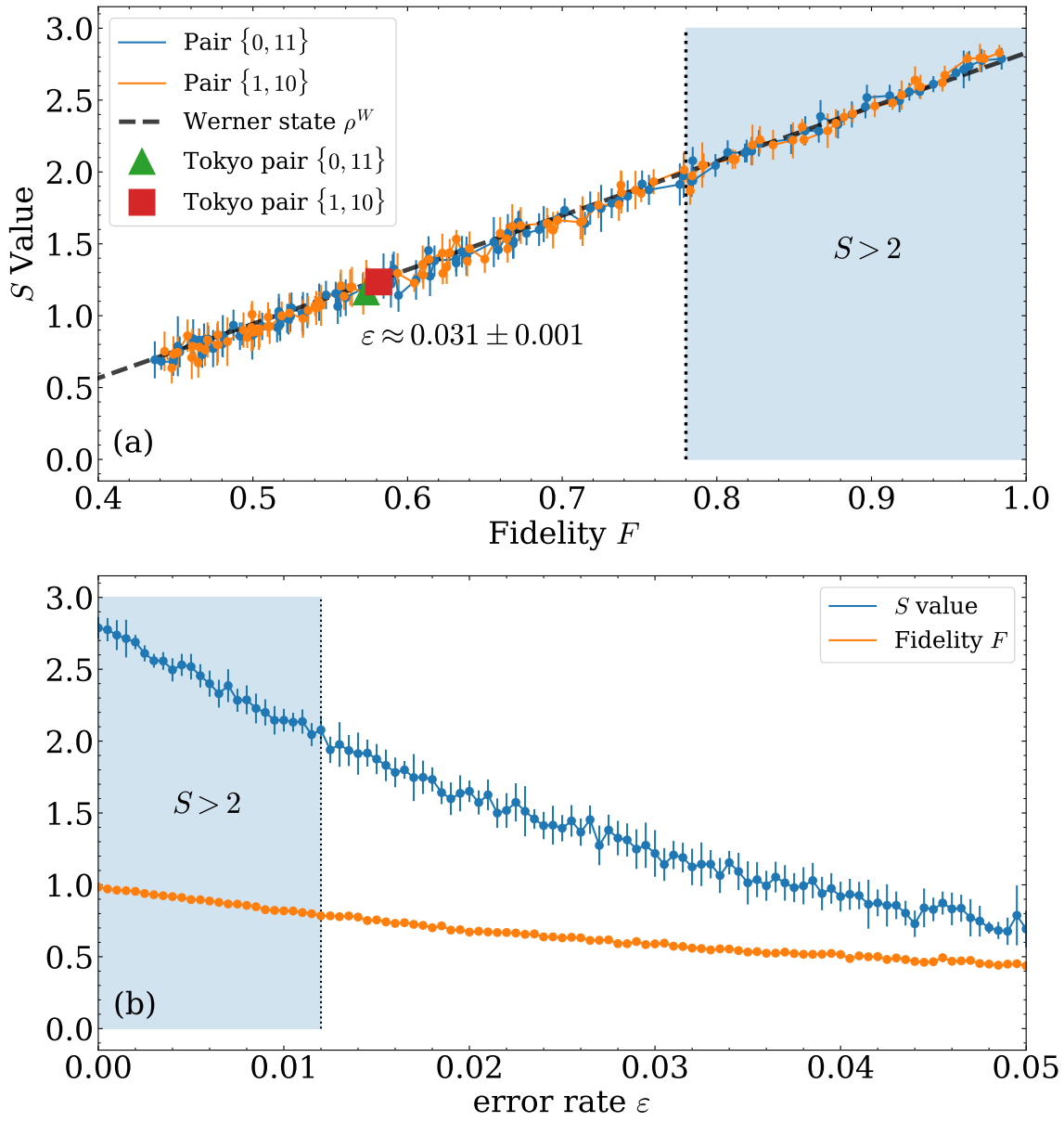

Figure 3-7: Simulation of the protocol using Qiskit QASM simulator [9]

The simulation vary probability of an error ϵ of single qubits operation O from 0 to 0.05 (10 times repeated for 101 data point and 1024 shots per point) and total

error of two qubits gate as two independent error on control and target qubits.

Rotated Werner state violates CHSH inequality when its fidelity $F \gtrsim 0.78$ (dashed line in figure[3-7]) as agree as our simulation data (blue point for $\{0, 11\}$ and orange point for pair $\{1, 10\}$ in figure[3-7]). Furthermore, the data points obtained from IBM Q 20 Tokyo (triangle point for pair $\{0, 11\}$ and square point for pair $\{1, 10\}$ in figure[3-7]) are fit well with the theoretical and simulation result. The simulation result suggest that the acceptable error rate ϵ which allow the protocol to violate CHSH inequality is $\epsilon \approx 1.2\%$ while its also implied that error rate of real data point has $\epsilon \approx 0.031 \pm 0.001$.

Chapter 4

Quantum Network Analyzer

A quantum network analyzer (QNA) is a simulation software of a quantum network on the platform of web-application. In a current version, QNA will serve as a tool for visualization of a network of qubits. It is capable of simulating a quantum teleportation protocol, such as measurement-based quantum network coding (MQNC).

As mentioned in Section 2.3, a quantum network represents a network of quantum devices, where each node represents a qubit or a quantum repeater or a quantum computer. Users can view the simulation, its dynamics, after each local operations, and they can try it and see it in graphics. Users can also construct any desired topology of a quantum network, and perform Pauli measurements on any node to transform the topology of the graph from one to another. The simulation uses classical operations on graph states that are equivalent to Pauli-measurements in order to simulate the protocol. Thus, matrix representation grows linearly with the number of nodes, so that the simulation can be carried out up to thousand quantum nodes. QNA is aimed to provide an analysis over graph states for both ideal and noisy cases. For a noisy case, the noise of operation can view as a success probability of operation, i.e. fluctuation can be added to Pauli measurement operators.

Ideally, users can choose any pairs on a graph network. Then QNA will give an analysis of possible path with series of operations that minimizes the resource used for achieve the final desired topology. This part is still a work in progress, as it relates to quantum control theory, and trajectory optimization. Both of these topics

are relatively new and being investigated extensively in literature [3, 11].

4.1 Framework

In this section, we aim to provide information about clickable application version of QNA using MQNC.

In order to classically simulate the MQNC protocol, we have to represent a cluster state in terms of a graph state. Fortunately, graph theory has operations equivalent to Pauli measurements. This is achieved by a series of local complementation and deletion on nodes as detailed in Section 2.3.2. We use python as programming language back-end. Networkx package represent the quantum network and using alcpack package to handle local complementation operations. The most difficult part is to create a front-end of the application which allows for visualization and users to interact with the quantum network. Dash is a python package that utilizes flask, a light weight python server package, and cytoscape JavaScript, an interactive network visualization together. We can easily create an web application with dash as a front-end and networkx combines with alcpack as a back-end.

4.2 Capability

QNA can generate a random geometry of a graph up to 200 nodes, comparing to the QASM simulator which allows to simulate a quantum network of around 20 nodes or up to 32 qubits using IBM Q QASM Simulator on cloud server. This is a significant improvement in terms of a size of the network. However, the drawback is that we cannot simulate the protocol with noise to evaluate the protocol in terms of a noise resiliency.

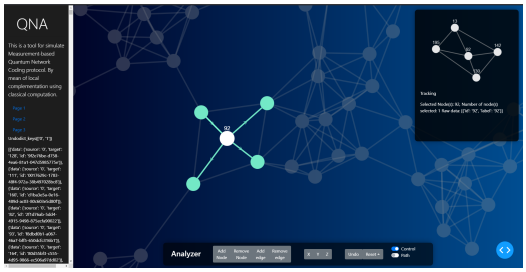

(a) The graph before applying Y-measurement on white node

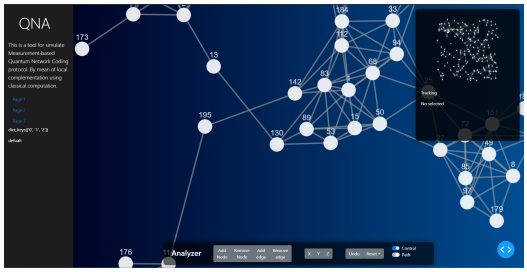

(b) The graph after applying Y-measurement on white node

Figure 4-1: Y-measurement on graph state

4.3 Entanglement Recreation

One can use QNA to reproduce the results of X-measurements on a bottleneck of the butterfly network to create two crossing-over entangled pairs following the procedure below.

1. Assuming initial six qubits in a butterfly network as in figure 4-2a where the qubits $\{0, 1\}$ are the bottleneck nodes. The goal is to generate direct entanglement link for pairs $\{2, 3\}$ and $\{4, 5\}$.

2. The first X-measurement is performed on the qubits $\{0\}$, while the qubit $\{3\}$ is selected as a feed-forward target qubit, as illustrated in a figure 4-2b and resulting in figure 4-2c.

3. The second X-measurement is performed on the qubit $\{1\}$. Here, again the qubit $\{3\}$ is selected as a feed-forward target qubit as illustrated in figure 4-2d. Thus, the goal is achieved as shown in figure 4-2e.

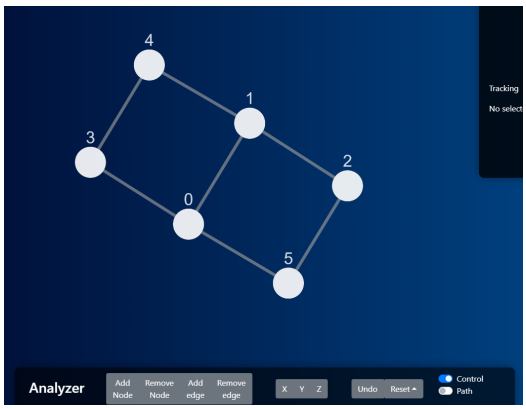

(a) Initial resource

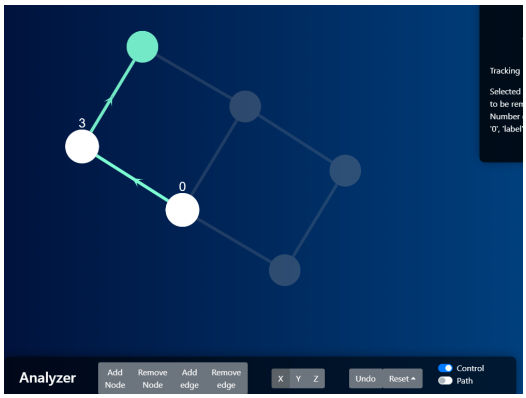

(b) X-measurement on node 0 and feed-forward target is node 3

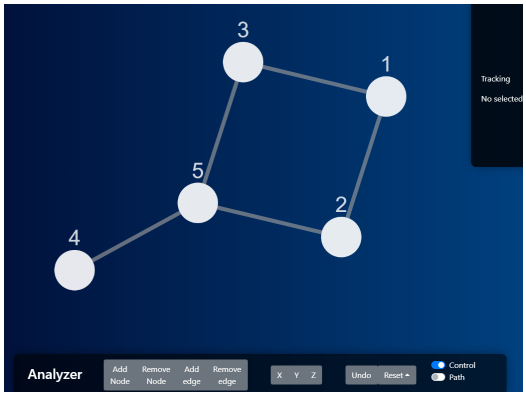

(c) The resulting network after X-measurement on node 0

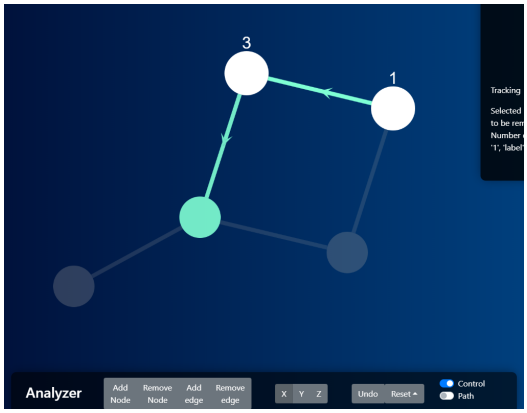

(d) X-measurement on node 1 and feed-forward target is node 3

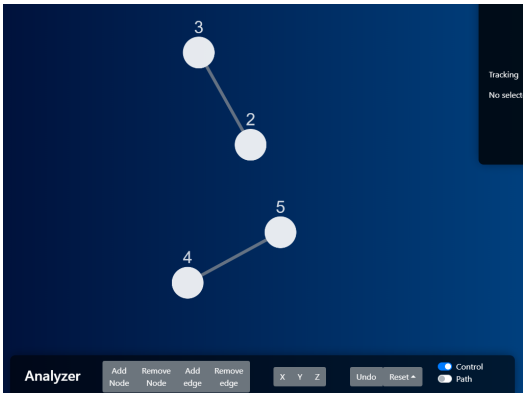

(e) The resulting network after X-measurement on node 1

Figure 4-2: Creation of 2 crossing-over entangle pair using sequence of X-measurement

Chapter 5

Conclusion

In the quest of establishing a quantum internet, minimization of the resource used is one of the main interest in this quest. Our research focused on investigating of the performance of measurement-based quantum network coding (MQNC), the protocol that is capable to overcome a contention problem in order to minimize time to link to distant nodes in a complex quantum network. MQNC uses local Pauli measurements instead of Bell-measurements which allow the protocol to have more flexibility in terms of transforming topology of a quantum network. As quantum computing and quantum communication are being realized more practically in research and applications, investigation on a quantum network has attracted increasing interests and become a vibrant and active field.

We implemented MQNC on a superconducting quantum processor to evaluate the quality of the entangled states that the protocol can generate. The two crossing-over qubits of a linear cluster state have fidelity $F \approx 0.57 \pm 0.01$ and $F \approx 0.58 \pm 0.01$, which are still lower than desirable. After turning a linear cluster state to a Bell-pair, the CHSH experiment showed that the S value of the generated Bell pairs did not exceed 2 in order to demonstrate a violation of the CHSH inequality. This implies that the desired entanglement is not guaranteed. However, the concurrence of each pair showed that entanglement possibly occurs in the generated Bell pairs. A main reason for this entanglement prevent can be accounted for by noise in the system.

Our simulation suggested that MQNC could distribute usable Bell-pairs over a

bottleneck network when the one-qubit error rate $\epsilon < 1.2\%$. This imposes upper bound on noise in a device which will allow the implementation of MQNC on the network. Unfortunately, for the device used in this work, the one-qubit error rate is approximately $\epsilon \approx 3.1\%$. In the future, such noise can be mitigated or suppressed, and our MQNC can be realized a real quantum network.

Based on local measurements and graph states of a quantum network, we have created a quantum network analyzer (QNA), a software which can serve as a useful tool for quantum network education with a nice interface. Thus far, QNA has features to operate specific local measurements, and display graphic representation of a quantum network. We will continue to improve it to analyze a quantum network such as the effect of noise from a single node on the network state, or an optimal control sequence to yield a desirable entangled pair. This is work in progress.

We hope that our research can contribute to the quest to build a quantum internet in the near future.

Bibliography

[1] A. Bouchet. Recognizing locally equivalent graphs. *Discrete Mathematics*, 114(1):75 – 86, 1993.

[2] H.-J. Briegel, W. Dür, J. I. Cirac, and P. Zoller. Quantum repeaters: the role of imperfect local operations in quantum communication. *Physical Review Letters*, 81(26):5932, 1998.

[3] S. Cong. *Control of Quantum Systems: Theory and Methods*. Wiley, 2014.

[4] W. Dür, H.-J. Briegel, J. I. Cirac, and P. Zoller. Quantum repeaters based on entanglement purification. *Phys. Rev. A*, 59:169–181, Jan 1999.

[5] A. G. Fowler, D. S. Wang, C. D. Hill, T. D. Ladd, R. Van Meter, and L. C. L. Hollenberg. Surface code quantum communication. *Phys. Rev. Lett.*, 104(18):180503, May 2010.

[6] M. Hein, W. Dür, J. Eisert, R. Raussendorf, M. V. den Nest, and H. J. Briegel. Entanglement in graph states and its applications, 2006.

[7] L. Jiang, J. M. Taylor, K. Nemoto, W. J. Munro, R. Van Meter, and M. D. Lukin. Quantum repeater with encoding. *Phys. Rev. A*, 79(3):032325, Mar 2009.

[8] T. Matsuo, T. Satoh, S. Nagayama, and R. Van Meter. Analysis of measurement-based quantum network coding over repeater networks under noisy conditions. *Phys. Rev. A*, 97:062328, Jun 2018.

[9] P. Pathumsoot, T. Matsuo, T. Satoh, M. Hajdušek, S. Suwanna, and R. Van Meter. Modeling of measurement-based quantum network coding on a superconducting quantum processor. *Phys. Rev. A*, 101:052301, May 2020.

[10] R. Raussendorf, D. E. Browne, and H. J. Briegel. Measurement-based quantum computation on cluster states. *Phys. Rev. A*, 68:022312, Aug 2003.

[11] L. Viola, E. Knill, and S. Lloyd. Dynamical decoupling of open quantum systems. *Phys. Rev. Lett.*, 82:2417–2421, Mar 1999.

[12] M. Zwerger, A. Pirker, V. Dunjko, H. J. Briegel, and W. Dür. Long-range big quantum-data transmission. *Phys. Rev. Lett.*, 120:030503, Jan 2018.